Originally published in: Physiological Measurement, 2009, 30: 869-883.

The definitive publisher authenticated version is available online at
doi: 10.1088/0967-3334/30/9/001

Vessel calibre and haemoglobin effects on pulse oximetry

M P M[c]Ewen[1, 2], G P Bull[2] and K J Reynolds[1]

[1] School of Computer Science, Engineering & Mathematics, Flinders University, Adelaide, Australia

[2] Flinders Biomedical Engineering, Flinders Medical Centre, Adelaide 5042, Australia

E-mail: Mark.McEwen@flinders.edu.au

Abstract

Despite its success as a clinical monitoring tool, pulse oximetry may be improved with respect to the need for empirical calibration and the reports of biases in readings associated with peripheral vasoconstriction and haemoglobin concentration. To effect this improvement, this work aims to improve the understanding of the photoplethysmography signal - as used by pulse oximeters, and investigates the effect of vessel calibre and haemoglobin concentration on pulse oximetry.

The digital temperature and the transmission of a wide spectrum of light through the fingers of 57 people with known haemoglobin concentrations were measured, and simulations of the transmission of that spectrum of light through finger models were performed.

Ratios of pulsatile attenuations of light as used in pulse oximetry were dependent upon peripheral temperature and on blood haemoglobin concentration. In addition, both the simulation and in vivo results showed that the pulsatile attenuation of light through fingers was approximately proportional to the absorption coefficients of blood, only when the absorption coefficients were small. These findings were explained in terms of discrete blood vessels acting as barriers to light transmission through tissue.

Due to the influence of discrete blood vessels on light transmission, pulse oximeter outputs tend to be dependent upon haemoglobin concentration and on the calibre of pulsing blood vessels - which are affected by vasoconstriction/vasodilation. The effects of discrete blood vessels may account for part of the difference between the Beer–Lambert pulse oximetry model and empirical calibration.

Key words

absorption, attenuation, haemoglobin, hemoglobin, noninvasive, photoplethysmography, pulse oximetry, scattering, transmission, vasoconstriction

1 Introduction

Pulse oximeter outputs can be influenced by factors other than arterial haemoglobin oxygen saturation (S_aO_2): blood haemoglobin concentration has been shown to affect the accuracy of pulse oximetry (Severinghaus and Koh, 1990; Vegfors *et al.*, 1992); placing pulse oximeter probes close to large blood vessels can degrade performance (Mannheimer *et al.*, 2004; Vegfors *et al.*, 1992); temperature induced peripheral vasoconstriction has been associated with increased pulse oximeter readings (Hynson *et al.*, 1992; Sessler *et al.*, 1992; Schramm *et al.*, 1997; Talke and Stapelfeldt, 2006; Kelleher and Ruff, 1989); non-temperature-induced peripheral vasoconstriction and vasodilation have resulted in increases and decreases respectively, in pulse oximeter readings (Talke and Stapelfeldt, 2006).

Pulse oximeters determine the pulsatile component of attenuation from measurements of the pulsating intensity of red and infrared light that has passed through tissue. The ratio of pulsatile attenuations of red (A_R) versus infrared (A_{IR}) light is then used to determine S_pO_2 (pulse oximeter estimation of arterial haemoglobin oxygen saturation).

The pulsatile attenuation can be determined with equation (1) (Aoyagi, 2003):

$$A = Log\left(\frac{I_{max}}{I_{min}}\right) = \varepsilon\, c\, \Delta d\,, \tag{1}$$

where A is the pulsatile attenuation, I_{max} is the maximum intensity of transmitted light (at diastole), I_{min} is the minimum intensity of transmitted light (at systole), ε is the extinction coefficient, c is the concentration and Δd is the pulsatile change in light path length through blood.

The theoretical basis of pulse oximetry is described by a Beer-Lambert model which demonstrates how ratios of optical measurements carry information about haemoglobin oxygen saturation (Webster, 1997). With this model, pulsations are attributed to the change in blood volume from diastole to systole (Mannheimer, 2007; Mendelson, 1992; Alexander *et al.*, 1989), and S_pO_2 is calculated according to equation (2) (Mendelson and Kent, 1989; Webster, 1997):

$$S_pO_2 = \frac{\varepsilon_{Hb,R} - \varepsilon_{Hb,IR}\left(\frac{A_R}{A_{IR}}\right)}{\varepsilon_{Hb,R} - \varepsilon_{HbO,R} + \left(\frac{A_R}{A_{IR}}\right)\left(\varepsilon_{HbO,IR} - \varepsilon_{Hb,IR}\right)}, \tag{2}$$

where A_R is the pulsatile attenuation of red light, A_{IR} is the pulsatile attenuation of infrared light, $\varepsilon_{Hb,R}$ is the reduced haemoglobin extinction coefficient for red light, $\varepsilon_{HbO,R}$ is the oxygenated haemoglobin extinction coefficient for red light, $\varepsilon_{Hb,IR}$ is the reduced haemoglobin extinction coefficient for infrared light and $\varepsilon_{HbO,IR}$ is the oxygenated haemoglobin extinction coefficient for infrared light

Although the first pulse oximeters determined S_pO_2 in accordance with the Beer-Lambert model (Moyle, 1998), it is no longer used in practice because the conditions for its use, including homogenous non-scattering media and known light path lengths (Tremper and Barker, 1989; Mendelson, 1992), are not strictly met. Empirical calibration caters for this situation, and enables pulse oximeters to work accurately (Tremper and Barker, 1989; Mendelson, 1992; Teng and Zhang, 2004; Severinghaus and Naifeh, 1987).

The role of light scattering in violating the Beer-Lambert model conditions is widely acknowledged (Webster, 1997; Mannheimer, 2007; Fine and Weinreb, 1993; Alexander *et al.*, 1989). However the overall influence of scattering is uncertain, because Liu (Liu *et al.*, 1995) showed that the scattering coefficient of tubes made negligible difference to the overall absorption coefficient of static tissue phantoms, in near infrared light. Tissue inhomogeneity may contribute to the difference between the Beer-Lambert model and empirical pulse oximeter calibration, as evidenced by the influence of large blood vessels (Mannheimer *et al.*, 2004; Vegfors *et al.*, 1992) and the influence of tissue outside blood vessels (Yang *et al.*, 2007).

This work investigates the influence that discrete blood vessel calibre and total haemoglobin concentration (tH_b) have on pulse oximetry and the difference between the empirical versus Beer-Lambert model calibration curves (Webster, 1997).

One ramification of the Beer-Lambert model, as implied by equation 1, is that the pulsatile attenuation of different colours of light would be proportional to the haemoglobin extinction coefficients. Due to light scattering this does not quite occur (Webster, 1997; Mannheimer, 2007; Fine and Weinreb, 1993; Alexander *et al.*, 1989). However the influence of scattering is marginalized by absorption where the absorption coefficients for blood are large (Anderson and Sekelj, 1967). If the diameter and haemoglobin concentration of blood vessels can influence pulsations in light transmission, the effect will be largest with pulsations in strongly absorbed light.

In this paper, pulsations in the transmission of a wide spectrum of light through the fingers of people with known tH_b and finger temperatures, as an indication of vasoconstriction/vasodilation (Hahn and Shore, 1994) are examined. The transmission of those colours of light through finger models is simulated using a Monte Carlo (MC) technique, which included light scattering as well as absorption, and with Beer-Lambert law based modelling. In vivo testing and simulations indicated that pulse oximetry is influenced by the effects of blood being located within discrete vessels.

2 Methods

2.1 Photoplethysmography equipment

A custom photoplethysmography instrument was constructed to direct light from 11-light emitting diodes (LEDs) (centre wavelengths 454, 465, 500, 526, 591, 622, 656, 772, 806, 943 and 1200nm) onto a finger. These LEDs were chosen from those commercially available, to include wavelengths normally used in pulse oximetry (approximately 660 and 940nm (Mannheimer, 2007)) as well as encompassing parts of the spectrum where a wide range of absorption coefficients for the major components of blood (haemoglobin and water) occurred. Lenses were used to focus light from all the LEDs onto the same area on fingers. The intensity of light that transmitted through fingers was measured with two photodiodes (one sensitive to 454-943nm, the other sensitive to 1200nm light). Photodiodes were positioned closely together; however their centres were separated by 5mm. The effect of this anomaly was tested by including, the 5mm offset in simulations. The force exerted by the photoplethysmography instrument (2.5N) was applied evenly over most of the distal phalanx via curved finger adaptors, to avoid the blanching that can occur when force is applied over a flat surface (Teng and Zhang, 2004).

2.2 In vivo Patient testing

Ethics committee approval was obtained for performing tests on patients, who were selected on the basis that they were having blood extracted for haemoglobin analysis, and were willing to undergo non-invasive testing. Patients (25 males 32 females, mean age: 57±17) rested in a sitting or supine position during testing. The transmission of light from the 11 LEDs was measured for 10-20 seconds, through a finger. Pulse oximeter (Nellcor-N594) output was recorded from a finger on the opposite hand. Index fingers were used unless they had injuries, in which case middle or ring fingers were used. Three sets of measurements were recorded from each patient. The peripheral temperature was sampled once per patient using a digital thermometer (Digitech®, Sandy, Utah USA, model QM1538). The thermometer probe (K type thermocouple) was held between the thumb and the finger used for light transmission measurements.

2.3 Data processing

Light transmission measurements were recorded at 90 samples/sec. Data from some tests (approximately 15%) were excluded due to movement artefact. The pulsatile maxima and minima for each LED were extracted from recorded signals, pulsatile attenuation (equation 1) was calculated for each max/min pair, and averaged over all max/min pairs for each test on each patient. Pulsatile attenuation ratios (as used in equation 2) were calculated by dividing the pulsatile attenuation of light from one LED by that from a second LED.

2.4 Monte Carlo simulations

A MC simulation program for photon migration through three dimensional heterogeneous media (tMCimg (Boas *et al.*, 2002)) was used to simulate the transmission of the 11 colours of light through fingers. Each simulation was performed using 10^8 photons.

Finger models were generated using Matlab® (The Mathworks, Natick, MA, USA) at a resolution of 0·02mm per volume pixel (voxel) and consisted of a nominal 12mm diameter fingertip (Phesant, 1987; Saengchaiya and Bunterngchit, 2004) with an outer 0·2mm epidermal layer (Lee and Hwang, 2002), surrounding dermis, pulp and bone (Netter, 2003), and a series of blood vessels: Finger tips contain 3 or more 0·58±0·10mm diameter (when not pressurized) arteries which form U-shapes from the palmar to the dorsal surface (Strauch and de Moura, 1990). Finger artery diameters can increase by up to 100% when pressurized (Langewouters *et al.*, 1986), and when subjected to systolic/diastolic pressure fluctuations, diameters pulsate by approximately 4% (Langewouters *et al.*, 1986). Numerous superficial veins are present in finger tips, with diameters ranging from ≤0·4mm to ≥0·8mm (Smith *et al.*, 1991). Finger models contained 3 pairs of arteries, with diastolic/systolic diameters of 1·00/1·04mm, 0·96/1·12mm, 0·23/0·27mm and 0·11/0·13mm, and 12 superficial veins with diameters of 0·4mm (6) and 0·7mm (6). Arterial pulsations in the latter 3 models were large (approximately 18%), which was necessary for the 4th set of simulations, where pulsations were limited by the resolution of models (0·02mm). For each set of simulations, 3 separate models were used: arteries at diastole, arteries at systole (with the same overall finger diameter as the diastolic model), and arteries at systole (with the overall finger diameter slightly increased to maintain the same extra vascular area as the diastolic model).

Simulated light was incident upon the centreline of finger models, initially directed toward their centre. For simulations using 454-943nm light a detector was positioned on the opposite side of the finger model directly aligned with the source, and for simulations using 1200nm light an additional detector, positioned 5mm more proximally was used - to reproduce the 5mm offset between the detectors used for in vivo measurements.

Absorption and scattering coefficients and anisotropy factors for MC simulations were available for most but not all wavelengths used in this study, so interpolation and extrapolation were performed in some cases, as has been done for similar MC simulations (Peris *et al.*, 2007). The coefficients and factors used in simulations are listed in table 1.

Table 1. Absorption coefficients (μ_a) scattering coefficients (μ_s) and anisotropy factors (g) used in MC simulations of light transport through finger models. Absorption coefficients for blood determined for 130g/L tH_b and 40% H_{ct} and water fraction = 1-0·304H_{ct} (Yang *et al.*, 2007). S_vO_2 is the venous haemoglobin oxygen saturation.

			454 nm	465 nm	500 nm	526 nm	591 nm	622 nm	656 nm	772 nm	806 nm	943 nm	1200 nm
Dermis and finger pulp (Matcher *et al.*, 1997; Bashkatov *et al.*, 2005)		μ_a (mm^{-1})	0·16	0·15	0·12	0·13	0·08	0·06	0·05	0·04	0·04	0·03	0·05
		μ_s (mm^{-1})	10·6	10·5	10·1	9·8	9·1	8·9	8·6	7·8	7·6	7	6·1
		g	0·91	0·91	0·91	0·91	0·91	0·91	0·91	0·91	0·91	0·91	0·91
Epidermis (Bashkatov *et al.*, 2005; Mobley and Vo-Dinh, 2003)		μ_a (mm^{-1})	0·16	0·15	0·12	0·13	0·08	0·06	0·05	0·04	0·04	0·03	0·05
		μ_s (mm^{-1})	43	39·6	32·4	29·2	22·6	20·3	18·3	14·6	14·1	12·3	11
		g	0·75	0·75	0·76	0·77	0·79	0·80	0·81	0·84	0·85	0·89	0·90
Bone (Ugryumova *et al.*, 2004; Behari *et al.*, 1977; Firbank *et al.*, 1993)		μ_a (mm^{-1})	0·13	0·14	0·15	0·12	0·07	0·06	0·05	0·03	0·03	0·02	0·02
		μ_s (mm^{-1})	35	35	35	35	34·1	33·7	33·1	29·8	29·5	26·1	24
		g	0·91	0·91	0·91	0·91	0·92	0·92	0·92	0·92	0·93	0·94	0·94
Blood (Anderson and Parrish, 1981; Suzaki *et al.*, 2006; Takatani and Graham, 1979; Zijlstra *et al.*, 2000; Cope, 1991; Palmer and Williams, 1974; Mobley and Vo-Dinh, 2003; Lovell *et al.*, 1999; Yaroslavsky *et al.*, 1996; Hammer *et al.*, 2001)	Arterial (97% S_aO_2)	μ_a (mm^{-1})	25·3	17·5	9·51	15·2	6·95	0·42	0·2	0·33	0·42	0·64	0·15
		μ_s (mm^{-1})	86·1	85·7	84·2	83·1	80·3	78·9	77·5	72·5	69	65	65
		g	0·97	0·97	0·97	0·97	0·98	0·98	0·98	0·99	0·99	0·99	0·99
	Venous (60% S_vO_2)	μ_a (mm^{-1})	21·7	13·6	8·94	14·6	8·95	1·14	0·72	0·44	0·41	0·54	0·14
		μ_s (mm^{-1})	86·1	85·7	84·2	83·1	80·3	78·9	77·5	72·5	69	65	65
		g	0·97	0·97	0·97	0·97	0·98	0·98	0·98	0·99	0·99	0·99	0·99

For each simulation, the intensity of light reaching the detector was calculated from the history file output of the MC simulation program, as described by Boas (Boas *et al.*, 2002). For each diastole/systole pair of simulations, the pulsatile attenuation of light was calculated according to equation 1.

2.5 Sums of light transmission along multiple parallel paths

The pulsatile light transmission through finger models was approximated by summing the light transmission, without scattering, along multiple paths throughout finger model cross sections. These "straight transmission sums" were calculated on the finger models used in MC simulations as well as finger models with varying tH_b (60-180g/L), S_aO_2 (0%-100%) and artery diameters (0·1-1·00mm at diastole, 4% larger at systole). Absorption coefficients for arterial blood, for these sums, were determined according to equation (5) using the extinction coefficients for oxygenated and reduced haemoglobin, and absorption coefficients for water (figure (3)), together with the relationship between tH_b (g L^{-1}) and H_{ct} (Habibzadeh *et al.*, 2001)

$$H_{ct} = \frac{tH_b}{330}, \tag{3}$$

and the relationship between H_{ct} and B_{wf} (whole blood water fraction) (Yang *et al.*, 2007)

$$B_{wf} = 1 - 0 \cdot 304 H_{ct}. \tag{4}$$

$$\mu_a = \frac{tH_b}{wt_{Hb}}\left(\left(S_a 0_2\right)\varepsilon_{HbO} + \left(1 - S_a 0_2\right)\varepsilon_{Hb}\right) + B_{wf}\mu_{a,water}, \tag{5}$$

where $\mu_{a,water}$ is the water absorption coefficient and wt_{Hb} is the H_b molecular mass (64585 (Moyle, 1998)).

The transmission of light through finger models was calculated using Matlab® at every 0·001mm through the cross section, in accordance with the Beer-Lambert law, as shown in equation 6 (Mobley and Vo-Dinh, 2003):

$$T = e^{-\mu_a d} \tag{6}$$

The overall light transmission, at diastole and systole, was calculated as the sum of all the individual transmissions, and used to determine the pulsatile attenuation of light in accordance with equation 1.

3 Results

3.1 In vivo testing: Temperature

The pulse oximeter tended to display higher S_pO_2 values for people with cold hands (figure 1), as also found by Hynson (Hynson *et al.*, 1992), Schramm (Schramm *et al.*, 1997) and Kelleher (Kelleher and Ruff, 1989).

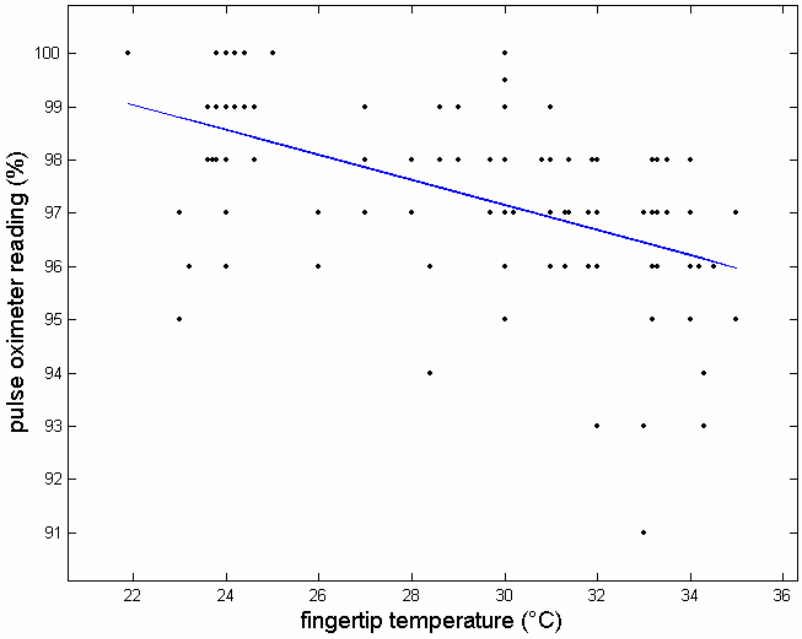

Figure 1. Pulse oximeter reading compared to peripheral temperature (sampled in the opposite hand). Correlation coefficient = 0·53, $p < 0{\cdot}01$.

3.2 In vivo testing: Haemoglobin

At the normal S_pO_2 values used in this study, no significant relationship between tH_b and S_pO_2 was found. However, there were statistically significant relationships between tH_b and ratios of pulsatile attenuations of light from several pairs of LEDs (eg figure 2).

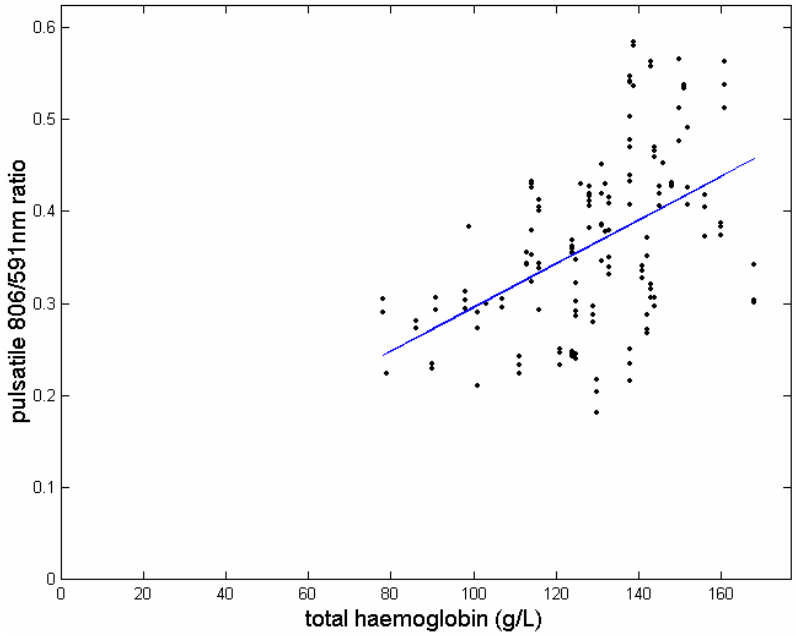

Figure 2. Relationship between the 806/591nm pulsatile attenuation ratio and tH_b. Correlation coefficient = 0·5, $p < 0{\cdot}01$, n = 146.

3.3 In vivo testing: Measured pulsatile light transmission through fingers

The mean pulsatile attenuation of light, for in vivo tests (figure 3), was approximately proportional to the extinction/absorption coefficients of haemoglobins and water at wavelengths longer than 600nm, but not at shorter wavelengths.

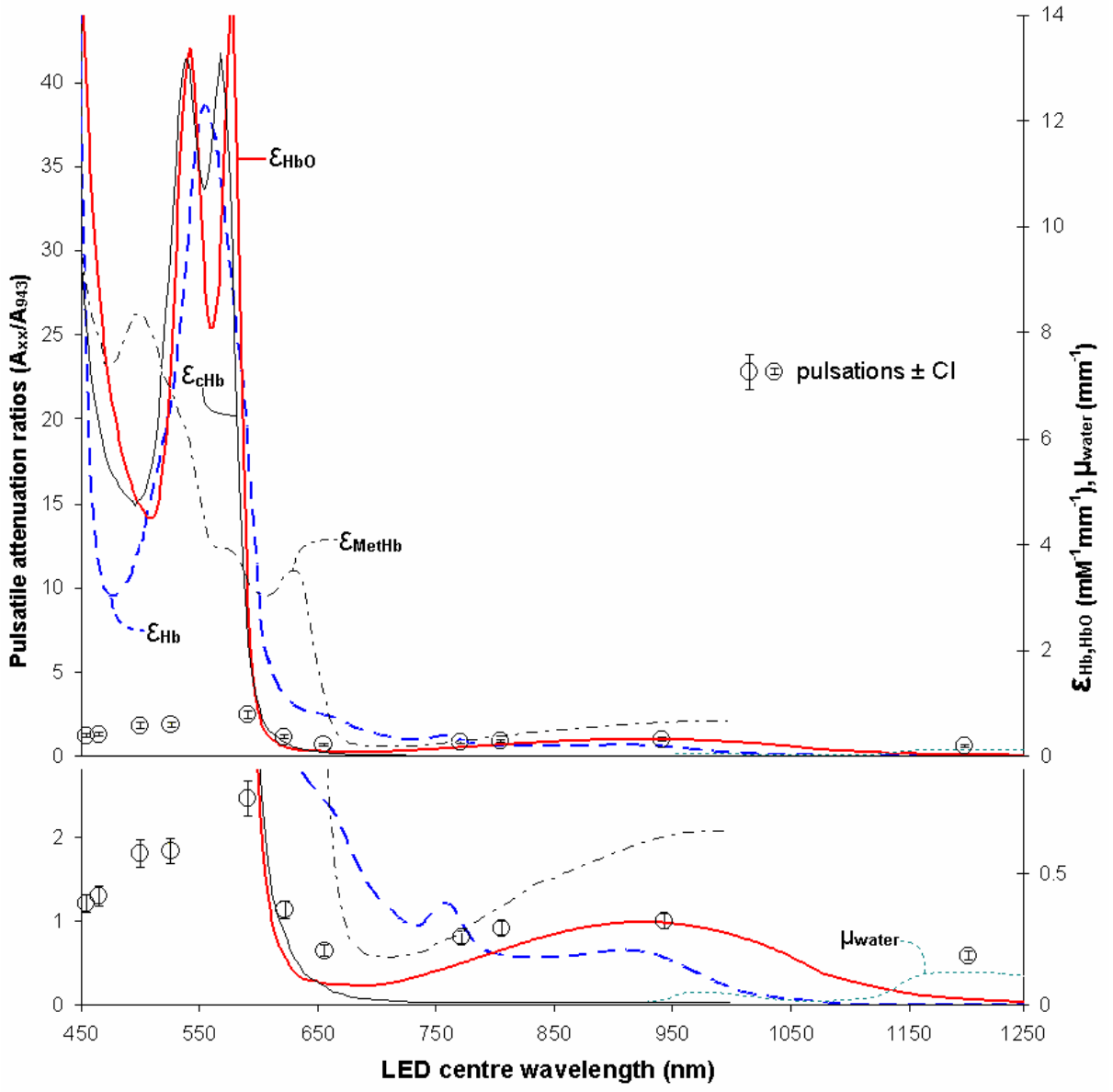

Figure 3. Mean (n = 146) measured pulsatile attenuation of light from each LED (calculated according to equation 1) normalized to the pulsatile attenuation of 943nm light. Pulsations shown in relation to the haemoglobin extinction spectra (Anderson and Parrish, 1981; Cope, 1991; Zijlstra *et al.*, 2000; Suzaki *et al.*, 2006) and water absorption spectrum (Buiteveld *et al.*, 1994; Palmer and Williams, 1974; Kou *et al.*, 1983). Error bars show 95% confidence interval (95% CI = 1·96*standard deviation/√n).

3.4 Simulated pulsatile light transmission through fingers

MC simulation results and straight transmission sums differed slightly from the in vivo results, but the lack of proportionality between pulsatile attenuations and absorption coefficients at wavelengths shorter than 600nm was similarly evident in all results (figure 4 pane a). As artery calibre decreased (panes b, c and d) the pulsatile attenuation of light tended to become more proportional to the haemoglobin extinction coefficients.

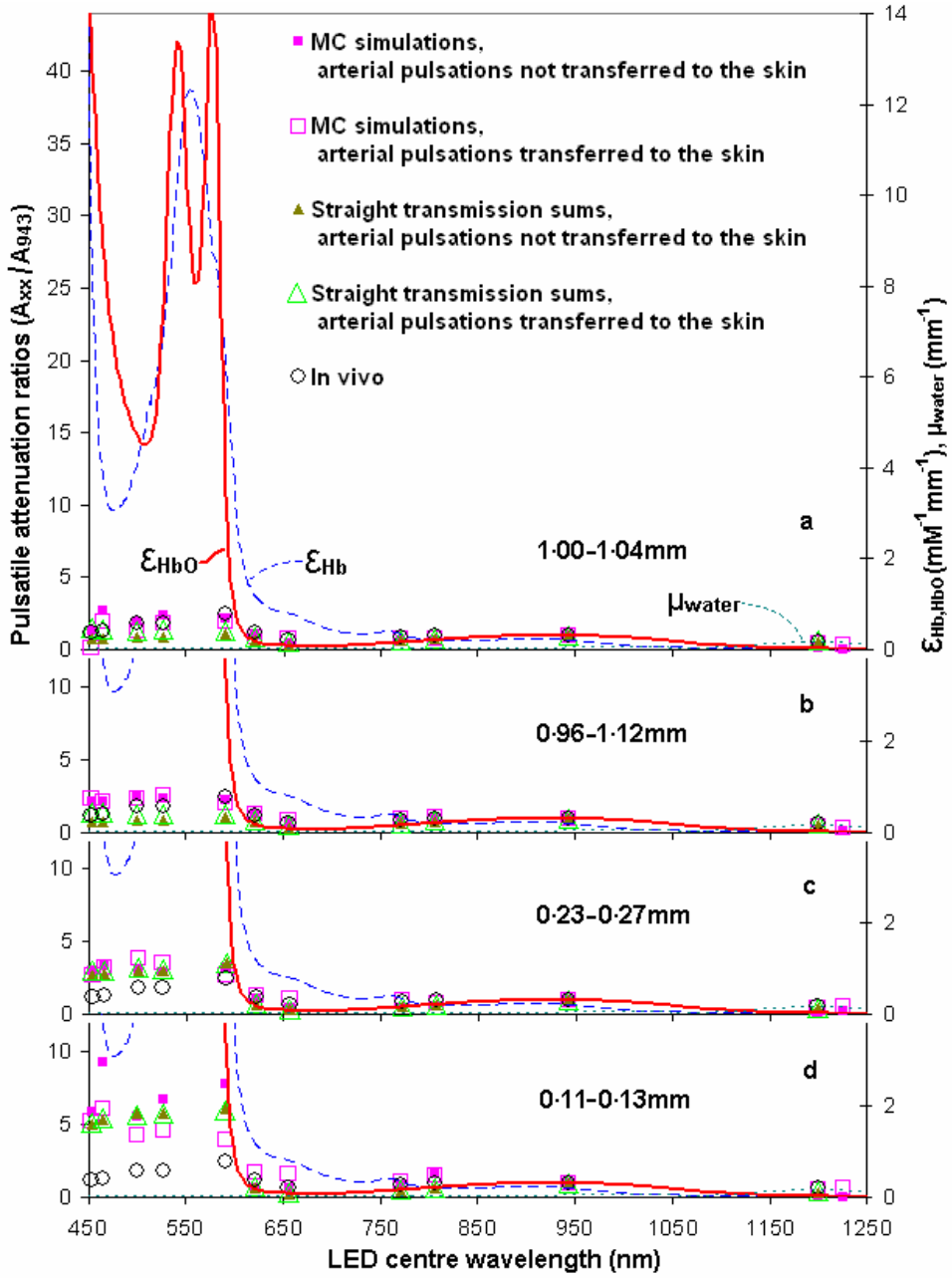

Figure 4. Results of MC simulations and straight transmission sums, compared to in vivo results and the haemoglobin and water absorption coefficients. Artery diameters pulsed (diastole to systole): 1·00-1·04mm (a), 0·96-1·12mm (b), 0·23-0·27mm (c), 0·11-0·13mm (d). The pulsatile attenuation of light from each LED was normalized to the pulsatile attenuation of light from the 943nm LED. Monte Carlo simulation results using the 1200nm detector in the same position as the 454-943nm detector, are shown at 1225nm for clarity.

The spread of results from simulations became greater as pulsations in artery diameters decreased, this was most notable in pane d of figure 4, where the arteries only pulsed by 0·02mm (signal to noise ratio was lowest). Increasing the number of photons used in simulations could improve the signal-to-noise ratio, however the effect

of artery calibre can be seen in figure 4, so increasing the number of photons per simulation beyond 10^8 was not justified.

Similar results were obtained from models where the pulsation of arteries were and were not transferred to the skin, from models with large versus small pulsations in artery diameters (panes a and b of figure 4), and from models that did and did not include the 5mm offset in the location of the 1200nm detector.

The agreement between the results of both simulation methods, when only MC simulations included scattering, supports the finding of Liu (Liu *et al.*, 1995), that the scattering coefficient of phantom blood made negligible difference to the overall absorption coefficient of tissue phantoms.

3.5 Straight transmission sums using the pulse oximetry LED combination

Apart from being influenced by S_aO_2, the red/infrared pulsatile attenuation ratio, determined from straight transmission sums, was dependent upon artery calibre and tH_b, as shown in figure 5.

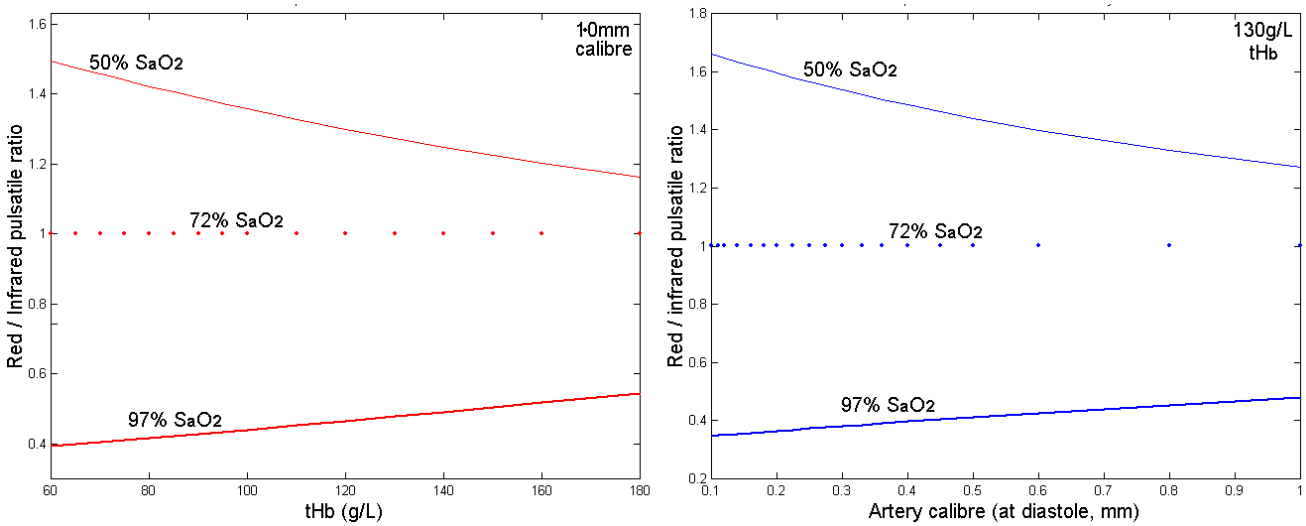

Figure 5. Red / infrared pulsatile attenuation ratio as tH_b varied (left pane), and as artery calibre varied (right pane) for straight transmission sums through finger models.

The relationship between the red/infrared pulsatile attenuation ratio and S_aO_2 (pulse oximetry calibration curve) was affected by artery calibre and tH_b (figure 6).

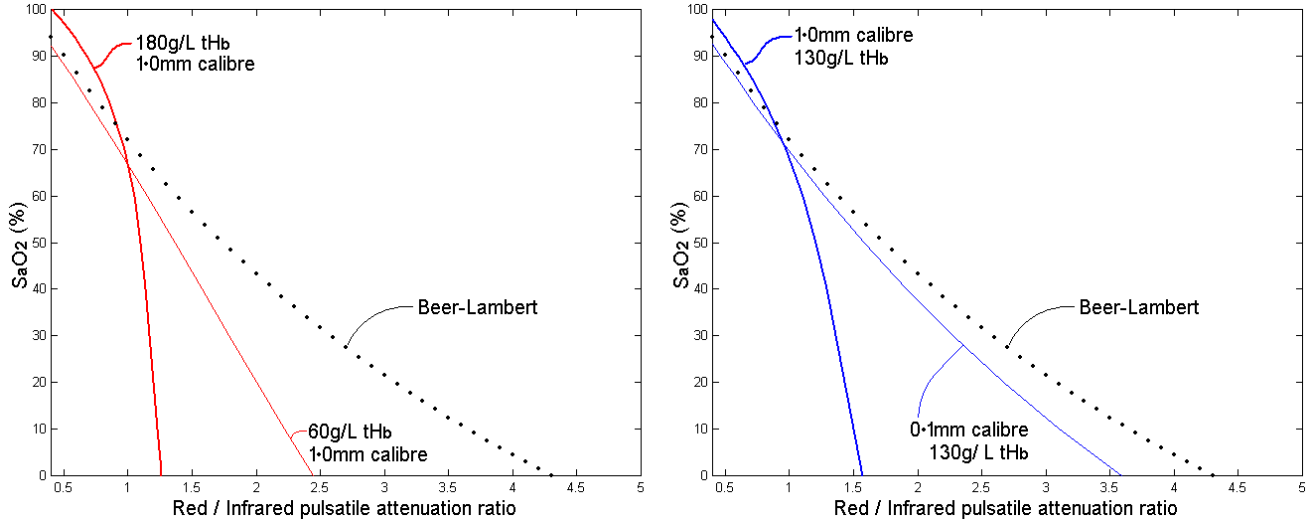

Figure 6. Effect of tH_b (left pane) and artery calibre (right pane) on the relationship between the red/infrared pulsatile attenuation ratio and S_aO_2, in straight transmission sums through finger models, compared to the Beer-Lambert pulse oximeter calibration curve (equation 2).

4 Discussion

The lack of proportionality between the absorption coefficients for blood and the pulsatile attenuation of 454-591nm light (figures 3 and 4) is caused by the same phenomenon as the nonlinear relationship found by Liu (Liu *et al.*, 1995) between the absorption coefficient (and diameter) of tubes and the overall absorption coefficient of the medium containing those tubes. The present study identifies that such nonlinear relationships are due to the range of pathlengths that arise when light interacts with discrete blood vessels, and shows how this can affect photoplethysmography and pulse oximetry.

4.1 Discrete blood vessel effects

Light scattering in blood is forward directed. This results in the average pathlength of light through a blood vessel, being related to the angle at which light enters the vessel. The shortest average pathlengths are associated with sharp angles to the boundary (figure 7) and the longest average pathlengths are associated with angles close to normal to the boundary.

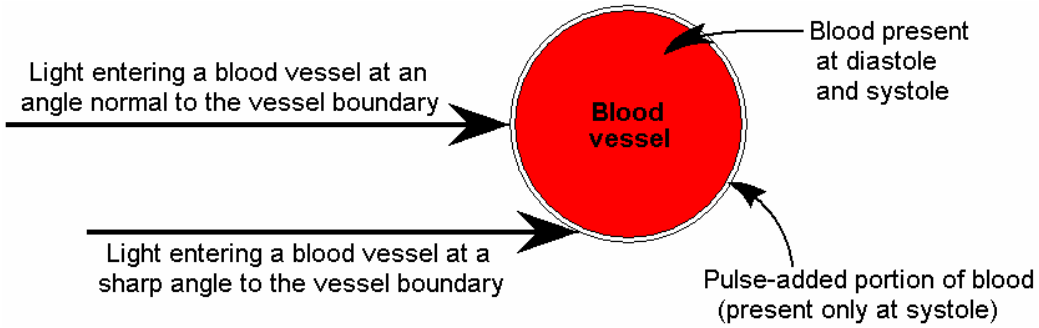

Figure 7. Light entering a blood vessel at normal and sharp (acute) angles to the boundary.

Light that interacts with the pulse-added portion (figure 7) contributes to pulsations in the intensity transmitting through tissue. However a major fraction of this light also interacts with the ever-present cylinder of blood in the centre of vessels, where it can be absorbed and prevented from contributing to pulsations. The amount of this absorption depends on the pathlengths of photons through the vessel. Due to the effects of multiple scattering and the angle of entry, the distribution of these pathlengths can be considerable. As pathlengths increase, transmission decreases (due to increased absorption), and this decrease is much more pronounced when absorption coefficients are large (eg 454nm light) than when they are small (eg 1200nm light). When absorption coefficients are large, only photons with short pathlengths through the ever-present cylinder of blood can survive to contribute to pulsations in light transmission through tissue. While weakly absorbed light with longer pathlengths can contribute to pulsations. Therefore whilst an increase in extinction coefficients tends to increase pulsations in light transmission in accordance with equation 1, it also tends to decrease the contribution to those pulsations made by photons with long pathlengths through the ever-present cylinder of blood. Hence, an increase in the absorption coefficient of blood will not result in a proportional increase in pulsatile light transmission and can, in fact result in a decrease in pulsatile transmission through tissue (when absorption coefficients become very large). This was the case for the in vivo test results (figure 3). Pulsations were smaller at 454nm than at 500nm, while the absorption of light by haemoglobin is larger at 454 than 500nm (figure 3).

4.2 Vessel calibre effects

When blood vessel calibre is large, the mean and longest photon pathlengths through vessels are generally greater than for small calibre vessels. Thus large calibre arteries will tend to decrease the contribution to light transmission pulsations made by photons interacting with the ever-present cylinder of blood, whilst small calibre arteries will tend to increase that contribution. This is demonstrated by the MC simulations and straight transmission sums through finger models, in figure 4. Simulated pulsations in light transmission through finger models tended to become more proportional to the haemoglobin extinction coefficients as artery calibre became smaller (panes b-d).

The influence of vessel calibre on S_pO_2, is dependent upon S_aO_2, because the effective extinction coefficient for haemoglobin $((S_aO_2)\varepsilon_{HbO} + (1-S_aO_2)\varepsilon_{Hb})$ is larger for red than infrared light when S_aO_2 is below approximately 72%, and is larger for infrared than red light when S_aO_2 is above approximately 72% (providing negligible dyshaemoglobins are present). Therefore small calibre arteries will tend to increase infrared light transmission

when S_aO_2 is above approximately 72%, more than they increase red light transmission. This results in a decrease in the red/infrared pulsatile ratio and an overestimation of S_aO_2. The opposite occurs when S_aO_2 is below approximately 72%; small calibre arteries will tend to cause S_pO_2 to underestimate S_aO_2. This is demonstrated with straight transmission sums through finger models with varying artery calibre (figure 5).

As artery calibre becomes larger, the pulsatile attenuation of light becomes less proportional to the absorption coefficient of blood (similar to the effect of large absorption coefficients). Hence, pulse oximetry (which relies on pulsations being approximately proportional to absorption coefficients) does not work properly near major arteries; This can explain the reports from Mannheimer – who found poor pulse oximeter performance when probes were positioned near large arteries (Mannheimer *et al.*, 2004), and Vegfors – who found that S_pO_2 was not related to S_aO_2 when probes were placed directly onto rabbit carotid arteries (Vegfors *et al.*, 1992).

4.3 Vasoactive effects

The transfer of blood volume pulsations to veins and venules due to thermoregulatory dilation of arteriovenous anastomoses has been proposed as a mechanism whereby temperature-induced peripheral vasoconstriction can indirectly influence pulse oximetry (Kelleher and Ruff, 1989; Hynson *et al.*, 1992; Schramm *et al.*, 1997). Whilst not discounting this mechanism, the present study identifies that vasoconstriction and vasodilation, even without the influence of arteriovenous anastomoses, can influence pulse oximeter readings, because the calibre of pulsing blood vessels affects the pathlengths of photons through those vessels, which affects pulsations in light transmission through tissue.

4.4 tH_b effects

The absorption coefficients of blood are dependent upon tH_b, hence tH_b can affect pulsations in the intensity of light transmitting through tissue, as evidenced by the relationships found between tH_b and ratios of pulsatile attenuation of light (eg figure 2). This can explain why tH_b has been reported to affect pulse oximetry. When analysing pulse oximeter readings, Severinghaus found that low tH_b was associated with underestimation of S_pO_2 - when S_aO_2 was low, and the influence of tH_b on S_pO_2 was small at normal S_aO_2 (Severinghaus and Koh, 1990). Similarly, the present study did not find a direct relationship between tH_b and in vivo S_pO_2 (only people with normal S_pO_2, were involved).

In the case of pulse oximetry, low tH_b tends to increase the red/infrared pulsatile attenuation ratio, when S_aO_2 is below approximately 72% – resulting in underestimation of S_aO_2. When S_aO_2 is above approximately 72% low tH_b tends to result in small overestimation of S_aO_2. These opposing outcomes are due to the effect of tH_b on S_pO_2 being dependent upon the effective extinction coefficient for haemoglobin, in the same manner as the effect of vessel calibre on S_pO_2 (section 4.2). The similar effects of tH_b and vessel calibre, on pulsatile ratios, can be seen in rabbit carotid artery tests (Vegfors *et al.*, 1992). Whilst applying pulse oximeter probes directly to arteries disrupted the relationship between S_pO_2 and S_aO_2, lowering haematocrit from 40% to 11% restored it (Vegfors *et al.*, 1992).

The paradox of tH_b having a strong effect on S_pO_2 when S_aO_2 is low and a small effect at normal S_aO_2, is due to; the shape of the pulse oximeter empirical calibration curve – which is flatter at high S_aO_2 than at low S_aO_2 (Tremper and Barker, 1989; Alexander *et al.*, 1989; Mendelson, 1992), as well as the relative values of ε_{HbO} and ε_{Hb}. In 940nm light $\varepsilon_{HbO,}$ is not substantially larger than ε_{Hb}, so whilst low tH_b will tend to increase pulsations in 940nm light (resulting in high S_pO_2 readings), this effect is not strongly dependent upon S_aO_2. The situation for 660nm light is different; $\varepsilon_{HbO,}$ is small while $\varepsilon_{Hb,}$ is relatively large. Therefore tH_b has a weak effect on pulsations in 660nm light when almost all haemoglobin is oxygenated, but when the fraction of reduced haemoglobin increases (low S_aO_2) low tH_b tends to allow greater transmission of 660nm light, which increases the 660/940nm pulsatile attenuation ratio, resulting in low S_pO_2 readings. The effect of tH_b on the 806/591nm ratio (figure 2), can be similarly explained: 806nm light is equally absorbed by oxy- and reduced haemoglobin, so although tH_b will affect pulsations in 806nm light this is independent of S_aO_2. At 591nm ε_{HbO} is large and ε_{Hb} is larger, therefore low tH_b tends to increase transmission of 591nm light, and this influence becomes greater as S_aO_2 becomes lower – resulting in a positive relationship between tH_b and the 806/591nm pulsatile attenuation ratio.

It must be noted that the relationships found between tH_b and pulsatile ratios, both in this study (eg figure 2) and as found by Severinghaus (Severinghaus and Koh, 1990) and Vegfors (Vegfors *et al.*, 1992) could be partly due to a light scattering phenomenon, because H_{ct} is related to tH_b (Habibzadeh *et al.*, 2001) and scattering is related to H_{ct} (Lovell *et al.*, 1999; Twersky, 1970).

4.5 Pulse oximeter calibration

The influence of discrete blood vessels may account for part of the difference between the Beer-Lambert model and pulse oximeter empirical calibration curves (Flewelling, 2000; Webster, 1997). Using straight transmission sums through finger models (figure 6) indicates that by modelling the light transmission through tissue with appropriate vessel diameters and tH_b, pulse oximeter calibration curves that are close to the Beer-Lambert model or close to empirical curves, can be produced.

5 Conclusions

The influence of absorption by blood, on pulsations in the light transmission through tissue, as used in pulse oximetry, is twofold. As the absorption coefficients of blood increase, pulsations in light transmission tend to increase - according to the Beer-Lambert law (modified by light scattering), and pulsations also tend to decrease - due to the influence of blood being located in discrete vessels. This study identifies the influence of discrete blood vessels as a mechanism that can explain some of the anomalies of pulse oximetry – namely why vasoconstriction and vasodilation, tH_b and the presence of large calibre blood vessels affect pulse oximetry.

The effects of discrete blood vessels may account for part of the difference between the Beer-Lambert pulse oximetry model and empirical calibration.

Due to the influence of discrete blood vessels, pulse oximeters that use the ratio of pulsations in 660nm and 940nm light will have outputs that are dependent upon the haemoglobin concentration and the diameter of pulsing blood vessels, which are affected by vasoconstriction / vasodilation. Vasoconstriction and low haemoglobin concentration both tend to generate erroneously low pulse oximeter readings when S_aO_2 is low, and tend to generate slightly high pulse oximeter readings when S_aO_2 is high. Vasodilation and high haemoglobin concentration tend to have the opposite effect.

6 References

Alexander C M, Teller L E and Gross J B 1989 Principles of pulse oximetry: theoretical and practical considerations *Anesth Analg* **68** 368-76

Anderson N M and Sekelj P 1967 Light-absorbing and scattering properties of nonhaemolysed blood *Phys Med Biol* **12** 173-84

Anderson R R and Parrish J A 1981 The Optics of Human Skin *J Invest Dermatol* **77** 13-9

Aoyagi T 2003 Pulse oximetry: its invention, theory, and future *J Anesth* **17** 259-66

Bashkatov A N, Genina E A, Kochubey V I and Tuchin V V 2005 Optical properties of human skin, subcutaneous and mucous tissues in the wavelength range from 400 to 2000 nm *JournaL of Physics D-Applied Physics* **38** 2543-55

Behari J, Guha S K and Agarwal P N 1977 Absorption spectra of bone *Calcif Tissue Res* **23** 113-4

Boas D A, Culver J P, Stott J J and Dunn A K 2002 Three dimensional Monte Carlo code for photon migration through complex heterogeneous media including the adult human head *Opt Express* **10** 159-70

Buiteveld H, Hakvoort J H and Donze M 1994 Optical properties of pure water *Proc. SPIE* **2258** 174-83

Cope M 1991 The application of near infrared spectroscopy to non invasive monitoring of cerebral oxygenation of the newborn infant In *Department of Medical Physics and Bioengineering, University College London* University of London pp 214-9

Fine I and Weinreb A 1993 Multiple scattering effects in transmission oximetry *Med Biol Eng Comput* **33** 709-12

Firbank M, Hiraoka M, Essenpreis M and Delpy D T 1993 Measurement of the optical properties of the skull in the wavelength range 650-950 nm *Phys Med Biol* **38** 503-10

Flewelling R 2000 Noninvasive Optical Monitoring In *The Biomedical Engineering Handbook* Bronzino J D ed CRC Press LLC: Boca Raton, Florida pp 86.1-11

Habibzadeh F, Yadollahie M, BSc M R and Haghshenas M 2001 Derivation of blood hemoglobin concentration from hematocrit:A simple method for rural areas *Archives of Iranian Medicine* **4** 120-2

Hahn M and Shore A C 1994 The effect of rapid local cooling on human finger nailfold capillary blood pressure and blood cell velocity *J Physiol* **478** 109-14

Hammer M, Yaroslavsky A N and Schweitzer D 2001 A scattering phase function for blood with physiological haematocrit *Physics in Medicine and Biology* **46** N65-9

Hynson J M, Sessler D I, Belani K, Washington D, McGuire J, Merrifield B, Schroeder M, Moayeri A, Crankshaw D and Hudson S 1992 Thermoregulatory vasoconstriction during propofol/nitrous oxide anesthesia in humans: threshold and oxyhemoglobin saturation *Anesth Analg* **75** 947-52

Kelleher J F and Ruff R H 1989 The penumbra effect: vasomotion-dependent pulse oximeter artifact due to probe malposition *Anesthesiology* **71** 787-91

Kou L, Labrie D and Chylek P 1983 Refractive indices of water and ice in the 0.65- to 2.5-μm spectral range *Applied Optics* **32** 3531-40

Langewouters G J, Zwart A, Busse R and Wesseling K H 1986 Pressure-diameter relationships of segments of human finger arteries *Clin Phys Physiol Meas* **7** 43-56
Lee Y and Hwang K 2002 Skin thickness of Korean adults *Surg Radiol Anat* **24** 183-9
Liu H, Chance B, Hielscher A H, Jacques S L and Tittel F K 1995 Influence of blood vessels on the measurement of hemoglobin oxygenation as determined by time-resolved reflectance spectroscopy *Med Phys* **22** 1209-17
Lovell A T, Hebden J C, Goldstone J C and Cope M 1999 Determination of the transport scattering coefficient of red blood cells *Proc. SPIE* **3597** 175-82
Mannheimer P D 2007 The light-tissue interaction of pulse oximetry *Anesth Analg* **105** S10-7
Mannheimer P D, O'Neil M P and Konecny E 2004 The influence of larger subcutaneous blood vessels on pulse oximetry *J Clin Monit Comput* **18** 179-88
Matcher S J, Cope M and Delpy D T 1997 In vivo measurements of the wavelength dependence of tissue-scattering coefficients between 760 and 900 nm measured with time-resolved spectroscopy *Applied Optics* **36** 386-96
Mendelson Y 1992 Pulse oximetry: theory and applications for noninvasive monitoring *Clin Chem* **38** 1601-7
Mendelson Y and Kent J C 1989 Variations in optical absorption spectra of adult and fetal hemoglobins and its effect on pulse oximetry *IEEE Trans Biomed Eng* **36** 844-8
Mobley J and Vo-Dinh T 2003 Optical Properties of Tissue In *Biomedical Photonics Handbook* Vo-Dinh T ed CRC Press pp 2.1-75
Moyle J T B 1998 *Pulse Oximetry* BMJ Books: London
Netter F H 2003 *Atlas of Human Anatomy* Icon Learning Systems: Teterboro, New Jersey
Palmer K F and Williams D 1974 Optical properties of water in the near infrared *J. Opt. Soc. Am.* **64** 1107-10
Peris V A, Hu S and Smith P R 2007 A Monte Carlo platform for the optical modeling of pulse oximetry *Proc SPIE* **6446** 64460T1-6
Phesant S 1987 *Ergonomics* British Standards Institution: London
Saengchaiya N and Bunterngchit Y 2004 Hand Anthropometry of Thai Female Industrial Workers *J of KMITNB* **14** 16-9
Schramm W M, Bartunek A and Gilly H 1997 Effect of local limb temperature on pulse oximetry and the plethysmographic pulse wave *Int J Clin Monit Comput* **14** 17-22
Sessler D I, McGuire J, Hynson J, Moayeri A and Heier T 1992 Thermoregulatory vasoconstriction during isoflurane anesthesia minimally decreases cutaneous heat loss *Anesthesiology* **76** 670-5
Severinghaus J W and Koh S O 1990 Effect of anemia on pulse oximeter accuracy at low saturation *J Clin Monit* **6** 85-8
Severinghaus J W and Naifeh K H 1987 Accuracy of response of six pulse oximeters to profound hypoxia *Anesthesiology* **67** 551-8
Smith D O, Oura C, Kimura C and Toshimori K 1991 The distal venous anatomy of the finger *J Hand Surg [Am]* **16** 303-7
Strauch B and de Moura W 1990 Arterial system of the fingers *J Hand Surg [Am]* **15** 148-54
Suzaki H, Kobayashi N, Nagaoka T, Iwasaki K, Umezu M, Takeda S and Togawa T 2006 Noninvasive measurement of total hemoglobin and hemoglobin derivatives using multiwavelength pulse spectrophotometry -In vitro study with a mock circulatory system *Conf Proc IEEE Eng Med Biol Soc* **1** 799-802
Takatani S and Graham M D 1979 Theoretical analysis of diffuse reflectance from a two-layer tissue model *IEEE Trans Biomed Eng* **26** 656-64
Talke P and Stapelfeldt C 2006 Effect of peripheral vasoconstriction on pulse oximetry *J Clin Monit Comput* **20** 305-9
Teng X F and Zhang Y T 2004 The effect of contacting force on photoplethysmographic signals *Physiol Meas* **25** 1323-35
Tremper K K and Barker S J 1989 Pulse oximetry *Anesthesiology* **70** 98-108
Twersky V 1970 Absorption and multiple scattering by biological suspensions *J Opt Soc Am* **60** 1084-93
Ugryumova N, Matcher S J and Attenburrow D P 2004 Measurement of bone mineral density via light scattering *Physics in Medicine and Biology* **49** 469-83
Vegfors M, Lindberg L G, Oberg P A and Lennmarken C 1992 The accuracy of pulse oximetry at two haematocrit levels *Acta Anaesthesiol Scand* **36** 454-9
Webster J G 1997 *Design of Pulse Oximeters* IOP Publishing Ltd: Philadelphia PA
Yang S, Batchelder P B and Raley D M 2007 Effects of tissue outside of arterial blood vessels in pulse oximetry: a model of two-dimensional pulsation *J Clin Monit Comput* **21** 373-9
Yaroslavsky A N, Yaroslavsky I V, Goldbach T and Schwarzmaier H-J 1996 Optical properties of blood in the near-infrared spectral range *proc SPIE* **2678** 314-24
Zijlstra W, Buursma A and van_Assendelft O 2000 *Visible and Near Infrared Absorption Spectra of Human and Animal Haemoglobin* VSP: Leiden, The Netherlands